ARTICLES
https://doi.org/10.1038/s41560-018-0136-x
nature energy

Planning for electric vehicle needs by coupling charging profiles with urban mobility

Yanyan Xu[1,6], Serdar Çolak[1,2,6], Emre C. Kara[3], Scott J. Moura[4] and Marta C. González[1,2,5*]

The rising adoption of plug-in electric vehicles (PEVs) leads to the temporal alignment of their electricity and mobility demands. However, mobility demand has not yet been considered in electricity planning and management. Here, we present a method to estimate individual mobility of PEV drivers at fine temporal and spatial resolution, by integrating three unique datasets of mobile phone activity of 1.39 million Bay Area residents, census data and the PEV drivers survey data. Through coupling the uncovered patterns of PEV mobility with the charging activity of PEVs in 580,000 session profiles obtained in the same region, we recommend changes in PEV charging times of commuters at their work stations and shave the pronounced peak in power demand. Informed by the tariff of electricity, we calculate the monetary gains to incentivize the adoption of the recommendations. These results open avenues for planning for the future of coupled transportation and electricity needs using personalized data.

The excessive exploitation of petroleum and coal affect not only the security of energy supply but also air quality and climate change. These shortcomings have triggered the search for cleaner alternative fuels for transportation[1–3]. Today's PEV technology is one of the most promising candidates to date[4,5]. The main issues that have hindered their adoption are: range anxiety, charger unavailability and high prices[3]. However, improvements in battery technology, tax breaks and subsidized charging programmes[6,7] have somewhat mitigated these limitations. As a result, PEVs are becoming a more viable means to move and are being adopted by drivers at steadily increasing rates[4]. According to the US Energy Information Administration, the number of PEVs in the United States doubled between 2013 and 2015 and is expected to reach 20 million by 2020[8].

Planning for the mobility needs of PEVs is particularly important in the context of the vulnerability of the power grid to outages that can cascade drastically[9]. Large-scale failures signified a need to reexamine the balance between power demand and the electricity infrastructure, opening the need for interdisciplinary approaches to study this complex system[10]. A body of literature has focused on the nature of network reliability of power grids, the role of network topology on the spread of cascading failures[11–17]. On the subject of PEVs and their impact on the grid, methods of optimization and control of PEV electricity consumption have a rich set of avenues[18–20]. Research topics on this front include measuring impact on the grid[21–27], developing accurate PEV energy consumption models[28], energy management[29,30], smart charging strategies that probe centralized and decentralized approaches[31,32], scheduling[33,34], peak shaving, emissions, pricing models[35,36] and joint optimization of power and transportation networks[37]. A common shortcoming in these works is the narrow scope in incorporating individual mobility needs into the analyses, often limited to the estimation of arrival or departure hours. Up-to-date data on individual mobility demand at metropolitan scale have not yet been incorporated into the planning schemes to manage electricity demand.

In this work, we target these gaps in the literature to extend the current knowledge of transportation-based electricity. For this purpose, we bring together three independent data sources: (i) mobile phone activity of a large sample of San Francisco Bay Area residents, (ii) charging sessions obtained from the commercial PEV supply equipment in the same region and (iii) surveys on the use of conventional and electric vehicles, together with census data for income information at the ZIP code level (see Methods). In the first part of the work, we estimate individual vehicular mobility per week day in the Bay Area using the mobile phone activity of a large sample of residents. We then present a Bayesian methodology to sample the PEV drivers from all travellers by utilizing information obtained from surveys regarding the household income and daily travel distances of PEV drivers. In the second part, with the charging session data, we analyse the various aspects of charging activity to characterize the nature of electricity demand at charging stations. We observe that PEV charging patterns are highly regular with morning and evening peaks following the traffic peaks. These peaks of demand are undesired because they can cause instabilities in the power grid. To tackle this problem, we explore the relationship between the electricity consumption of simulated PEV commuters working in the selected ZIP codes and the observed energy demand at individual commercial charging stations in the same region. We calibrate the charging behaviours of PEV drivers to match the observed demand. As an application, we lay out a charging scheme that minimizes the peak power by changing the start and end of the charging sessions, while also taking into account the constraints in changing departures and arrivals. We show how not knowing the mobility constraints decreases the potential of the peak minimization schemes. In contrast, introducing the awareness of individual mobility increases the feasibility of their adoption, affecting less the benefits of peak minimization. The resulting effects on the commuting travel times and the monetary benefits from the changes in charging times support the viability of the charging time shifts. Figure 1 depicts a summary of the proposed framework.

[1]Department of Civil and Environmental Engineering, Massachusetts Institute of Technology, Cambridge, MA, USA. [2]Lawrence Berkeley National Laboratory, Berkeley, CA, USA. [3]SLAC National Accelerator Laboratory, Menlo Park, CA, USA. [4]Department of Civil and Environmental Engineering, University of California, Berkeley, CA, USA. [5]Department of City and Regional Planning, University of California, Berkeley, CA, USA. [6]These authors contributed equally: Yanyan Xu and Serdar Çolak. *e-mail: martag@mit.edu

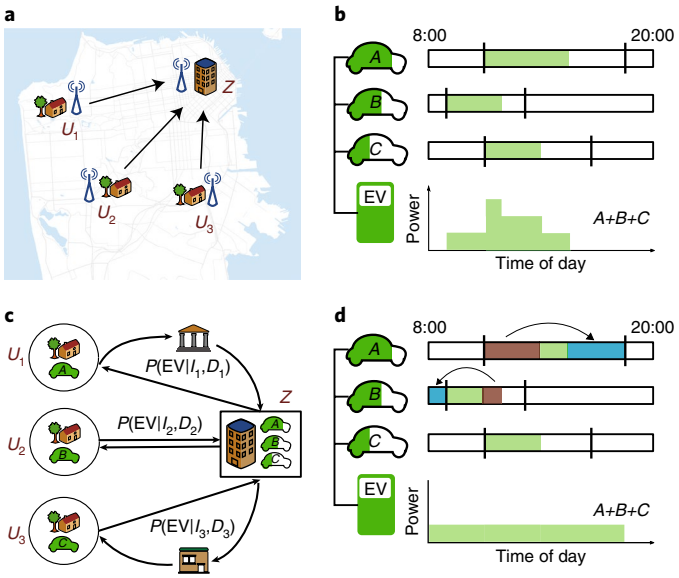

Fig. 1 | Coupling PEV charging with urban mobility. a, Mobile phone data are used to model individual mobility. Three users, U_1, U_2 and U_3, interacted with their mobile phone at their home and then at workplace Z. **b**, Charging sessions data are used to characterize individual and total electricity demand curves. The charging power per timeslot of vehicle A, B and C are 1 kW, and their charging sessions are overlapped. The green bar plot shows the total electricity demand of vehicle A, B and C at the charging station during one day. The peak electricity demand reaches 3 kW. **c**, The Bayesian inference method is proposed to find the probability that the vehicular trip is made by a PEV. **d**, Charging activity is shifted to create a recommendation scheme that relieves peaks in demand. The peak electricity demand at the charging station is reduced to 1 kW via shifting the charging sessions of vehicle A and B.

Estimating individual mobility of PEV drivers

We simulate the individual mobility of the entire population of the Bay Area using a fine-scale urban mobility model, TimeGeo[38]. This process begins with the extraction of stay locations in the trajectories of each individual[39–41]. Each stay is then accordingly labelled as home, work or other, based on temporal properties of the call activities. According to whether the workplaces are detected or not, we model the trips of commuters and non-commuters respectively (see Methods). Figure 2a represents the simulated trajectory and the labelled activities of a mobile phone user. The simulations of individual mobility based on mobile phone data compare very well with the results using two travel surveys, the 2010–2012 California Household Travel Survey (CHTS)[42] and the 2009 National Household Travel Survey (NHTS)[43]. As shown in Fig. 2b,d, the daily visited locations and fraction of departures per time of the day simulated by our model based on phone data agree well with the travel surveys. Further comparisons are presented in the Supplementary Figs. 1 and 2.

Mobility motifs[44] describe the individual daily travel networks, where nodes are visited locations and directed edges are trips from one location to another. For example, the motif of an individual whose only trips in a day are to and from work will consist of two nodes with two directed edges (one in both directions). On average, individuals visit three different places per day. When constructing all possible directed networks with six or fewer nodes, there exist over a million ways for an individual to travel between. However, 90% of people use one of just 17 networks, called motifs[44]. While nearly half of the population follow the simple two-locations motif. These results can be modelled with a probabilistic Markov model[38] that assigns particular rates to each individual informed by their trip behaviour. The top ten motifs of nearly six million simulated drivers in the Bay Area are summarized in Fig. 2c, which implies that the distribution of our simulated motifs agrees well with the information gathered from mobile phone users. The comparison of motifs of commuters and non-commuters are shown in Supplementary Fig. 1c.

After simulated individual mobility overall, we can probabilistically estimate the individual mobility of PEVs. To that end, we utilize the vehicle usage rate from the US census data and the California Plug-in Electric Vehicle Driver Survey[45]. According to this survey, PEV drivers' income distribution is skewed towards higher income segments. In particular, the percentage of those with average annual incomes above US$150,000 among conventional vehicle drivers is 15%, compared with the 47% observed among PEV drivers. The survey also highlights the typical distances PEV drivers travel: 64% of PEV drivers travel less than 30 miles per day (Table 1). This information is used to subsample PEV trips from total vehicular trips by implementing the Bayesian sampling procedure. Namely, we use the individual income estimated from the US census data at the census tract level and daily route distance from TimeGeo to estimate the probability of that the driver travels with a PEV, both for commuters and non-commuters (see Methods).

Figure 3a depicts the number of PEVs estimated from the Bayesian method at each ZIP code and the number obtained from the dataset on PEVs collected by the California Air Resources Board's Clean Vehicle Rebate Project[46], referred as the CVRP dataset. Figure 3b shows a good agreement between the number of PEVs obtained via the Bayesian estimates and the mobility model versus the ground truth of PEV usage. Figure 3c,d compares the distributions of the morning route distance, D, made by all commuters versus PEV drivers, as well as the commuting travel time, T, under free flow conditions. There are fewer PEV trips shorter than 5 km and longer than 25 km, in agreement with the findings of the survey. Figure 3e depicts the four mobility motifs from PEV commuters, showing that approximately 66% of PEV commuters mostly travel between home and work during weekdays. The simple motif (with ID = 1) is more prevalent among PEV drivers than among commuters using conventional vehicles, this may be a sign of the driver's concerns on the range of PEVs.

Electric vehicle charging session data profiles

In this section, we analyse PEV charging in non-residential regions by examining: visitation patterns and adoption rates, temporal features of arrivals and departures, and typical energy and power consumption levels. PEV drivers display varying degrees of regularity in terms of how often they visit charging stations. Figure 4a reveals that for the majority of PEV drivers the average number of charging sessions per day, N_{day}, is less than one. The bottom left inset in Fig. 4a displays the logarithmic distribution of the number unique PEV charging stations (EVSEs) visited by each PEV driver, N_{EVSE}. Noticeably, the great majority of PEV drivers (95.6%) is observed in less than 20 distinct EVSEs. The top right inset of Fig. 4a depicts the rate of PEV adoption observed throughout the year. The 3,000 drivers observed in January 2013 increases by an average of 1,000 per month, doubling twice over the course of 2013.

We look at the arrival and departure hours of charging sessions, h_a and h_d, in Fig. 4b. Approximately 50% of all arrivals take place in the 6:00–11:00 morning period, and as expected, the morning and the evening peaks are highly pronounced. This points to the parallels between the temporal component of overall travel demand to electricity demand. We compare the distribution of departure time in the morning of commuters with the arrival time of charging sessions and find notable delay between these two distributions (see Supplementary Fig. 6a). Such delay represents the driving time

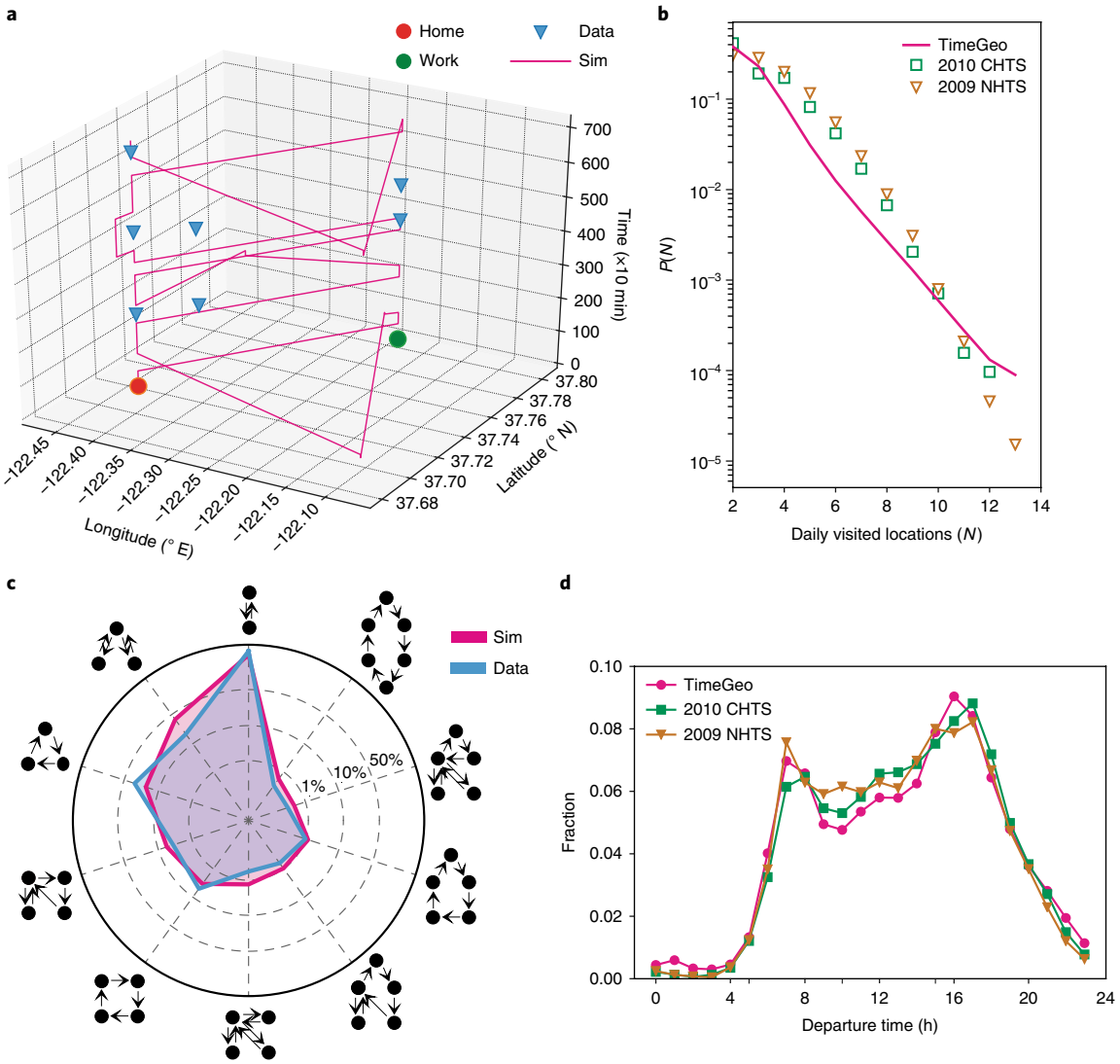

Fig. 2 | Validation of individual mobility simulation in the Bay Area. a, Simulated trajectory of a mobile phone user who is labelled as commuter. The blue triangles represent the actually recorded activities of the selected user from 22–25 October 2012. The red and green circles are the recognized home and work from the mobile phone data respectively. **b**, Population distribution comparison of daily visited locations between simulation and two travel survey datasets: 2010 CHTS and 2009 NHTS. Supplementary Fig. 1a,b presents comparisons of two more properties of mobility: stay duration (panel a) and trip distance (panel b). **c**, Validation of individual mobility motifs for a sample of mobile phone users in simulation and CDRs data. Nodes and directed edges in the label denote the visited locations in sequence during one day. 1%, 10% and 50% denote the values of the three dashed grid lines in the radar plot. The red-violet and blue shaded areas denote the fraction of the motifs in all users' travel activities observed from the CDRs data and the simulation, respectively. Around 65% of users observed only travel between two locations from the mobile phone data. The distribution of the ten primary motifs shows a high degree of similarity to the CDRs data. **d**, Fraction of trip departures by time of the day, comparing the simulation, the 2010 CHTS and the 2009 NHTS. Supplementary Fig. 2 shows the comparisons for various trip purposes.

of commuters from home to work in the Bay Area, which is around 30 min on average[47]. In the inset of Fig. 4b we look at the distribution of inter-arrival and inter-departure times, Δh_a and Δh_d, that is, the time between two consecutive charging sessions for the same driver ID. These distributions are peaked at multiples of 24 h, pointing to the diurnal periodicity of PEV drivers' charging behaviour. These findings reinforce the notion that commuting and charging behaviour in the non-residential regions are highly related.

Next, we shift our focus to measures per session, such as energy, duration and power. Figure 4c exhibits the average energy consumption per session, E_S. The battery sizes of Nissan Leaf (24 kWh) and Chevrolet Volt (16 kWh), two of the most commonly used PEVs in the region, are marked (see also Supplementary Fig. 4)[46]. Typically, E_S are well below these capacities, indicating that PEV drivers typically stay within the range of their PEVs. PEV drivers can charge at home or not necessarily start their commute at full capacity. On the other hand, the distribution of session durations reveals that 98.4% of all charging sessions last less than a day (Fig. 4c), in line with the ubiquitous charging at work places. Given the flexibility in terms of battery capacity and mobility patterns, here we assume that the session energy E_S represents not a single commuting trip, but rather a number of them.

The actual charging activity does not last as long as the session duration, δ_S, as seen in Fig. 4d. We divide sessions into four categories based on their session duration and plot the average power consumption for each segment at various percentages of the total duration. We observed three levels of power rate that are most common, denoted here as levels 1–3 (L1, L2 and L3). The first

Table 1 | Characteristics of PEV drivers

	Category	Conventional	PEV
Income (US$1,000)	Unknown	20%	17%
	<50	20%	2%
	50–100	30%	13%
	100–150	14%	20%
	>150	15%	47%
Distance (miles)	<15	-	14%
	15–30	-	50%
	30–45	-	28%
	>45	-	8%

Distribution of household income and the daily travelled miles of PEV drivers in California, USA[45].

two deliver 120 V and 240 V, typically corresponding to 3.3 kW and 6.6 kW, respectively. L3 chargers are mainly for fast charging at 480 V and are relatively uncommon. As faster charging technology becomes more abundant, the peak load yielded by PEVs will be even higher as the charging sessions start intensively in the morning. In the charging dataset, L1 and L2 chargers make up 99.9% of all the sessions in the dataset (see Supplementary Fig. 6d). This composition of power ratings explains the 4 kW upper limit to average power consumption observed in Fig. 4d. For sessions lasting less than 4 h, average power stays above 3 kW up to 80% of the duration of the session. Conversely, for sessions that last longer than 12 h but less than a day, only in the starting 25% of the session duration is there active charging. This corresponds approximately to 3–6 h, and the power remains zero thereafter. This is consistent with constant-current, constant-voltage battery charging behaviour and it suggests that currently there is no strategy to charging involved: PEVs are charged immediately on arrival.

Coupling PEVs energy demand and mobility patterns

This section presents the coupling of the individual mobility of PEV drivers with the energy demand at each destination. First, we measure the distribution of electricity demand at a ZIP code from the charging sessions, and connect that to the distribution of estimated energy demand of simulated PEVs commuting to that ZIP code. The charging sessions data is provided by a private company with a partial coverage of the market with reasonable agreement of the most popular destinations for charging (see Methods, and the comparison of estimated PEVs versus the charging data in Supplementary Fig. 5). To estimate the energy demand of each PEV trip, we first assign each PEV a mode from the four most popular modes (see Supplementary Fig. 4). Each PEV mode is associated an energy consumption model. Specifically, we use the drivetrain model for the two battery electric vehicle (BEV) modes, Nissan Leaf and Tesla Model S[48], and the charge-depleting model for the two plug-in hybrid electric vehicle (PHEV) modes, Chevrolet Volt and Toyota Prius[49]. For each PEV trip, we estimate the energy demand using its average speed and route distance (see Methods).

Due to the limited information from charging sessions data, we can not infer the state of charge of each vehicle. Therefore, we assign different shares of charging states: morning consumption, daily consumption and two-days consumption. This corresponds to different charging behaviours respectively: charging both at home and work every day, charging at work once per day or charging at work once every other day, indicating that the energy consumption at the arrival equals to the consumption of the trips in the last two days. In Fig. 3f, we show the comparison of probability distributions of the energy consumption of the three scenarios together with the actual charge, E_S, in a selected ZIP code. The peaks in the distribution of E_S demonstrate the heterogeneity in the electricity demand, which is mainly caused by the travel distance, the battery capacities and the charging behaviours of various PEVs. The 3–4 kWh peak, which can be observed in both actual and estimated consumptions, is a combination of low energy demand as a consequence of short commuting trips and PHEVs that typically have a battery capacity around 4 kWh (ref. [50]). Further comparisons between daily consumption estimates and the charging station data in selected ZIP codes are shown in Fig. 3g. The charging data have more pronounced peaks than our daily curves, this may be because our charging behaviours are simplified, leaving room for further improvements.

To estimate the charging behaviour in the given ZIP code, we limit the amount of charging sessions to 30 kWh. The charging behaviour is distributed to match the demand of the ZIP code with most charging sessions. Corresponding to average charging schemes that result in: 10%, 35% and 55% of the PEVs drivers, respectively (see also Supplementary Fig. 6c). Note that only 10% of the drivers charging at home is in agreement with a recent report by the Department of Energy, which states that 80% of partners in their Workplace Charging Challenge programme provide free PEV charging[51]. We randomly assign the charging speed from the charging session data to the simulated PEVs to make the distribution of charging speed match with the ground truth (see Supplementary Fig. 6d).

Strategies to mitigate peak demand with mobility needs

Our goal in this section is to transform the load curve into one that is more uniformly distributed across the day. To that end, we propose changes in the start and end of the charging sessions such that the peak power load is minimized. We cast the problem as a mixed-integer linear program with discrete shifts in arrival times and charging end times as inputs (see Methods). The program modifies the total power P_t measured through the day resulting from the overlapping charging activities of a population of PEVs in a way that minimizes the peak power while keeping the total energy consumed constantly. In this context, we test two different strategies. The first fixes the departure times for PEVs and shifts the arrival time in advance by d^i, an amount specific to session i within the interval $[0,d]$, to minimize the peak power load P_{peak}. We refer to this strategy as end bound. The second strategy, referred to as flexible, offers modifications to both of the arrival and departure times. In this approach, charging activity is shifted in the interval $[-d,d]$. In both of the two strategies, the PEVs are charged once they are plugged into the charging station and PEV driver could depart at their scheduled time if the charging session has finished. As a future scenario, we show the peak load saving when the charging station is able to control the start of the charging session independent of the arrival time. The current infrastructure does not allow the start of charging at an optimized time and it is coupled to the PEV arrival. With a smarter charging-shift scenario, the charging could be freely shifted between the plug-in/arrival and plug-out/departure time. We test the time shifting scenarios on the 448 PEVs travelling to our ZIP code with the largest number of incoming users.

Figure 5a illustrates an instance where 40 charging sessions in one day are shifted flexibly. Some users are recommended to charge earlier and others later than their actual request. Figure 5b depicts how the power curves are modified under the flexible strategy with varying value of d (Supplementary Fig. 7 presents the results for the end bound strategy). The flexible strategy reduces P_{peak} down 47% from 1,019 kW to approximately 479 kW for $d=4$, or 1 h. In contrast, the charging-shift strategy reduces the peak load by 66% as we have more room to operate the PEV charging.

We also evaluate the effects of introducing the constraints of the individual mobility motifs of each PEV. Mobility constraints are introduced via the four motifs depicted in Fig. 3e. More than 30% of PEV drivers have other activities before or after work,

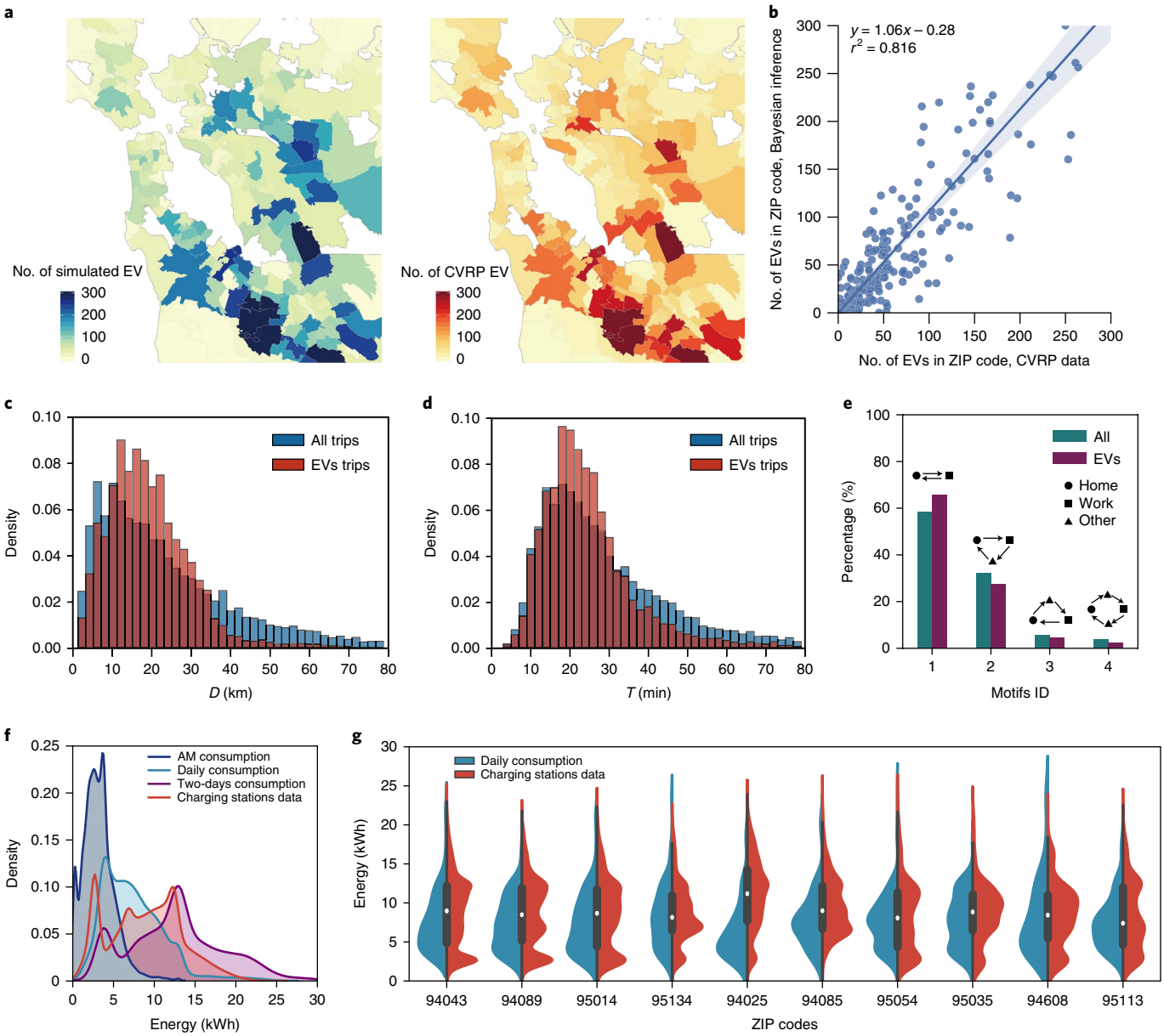

Fig. 3 | Validation of PEV mobility estimation and calibration of PEV charging behaviour. a, Number of PEVs in the residential ZIP codes of the Bay Area from the simulation and the CVRP datasets in the end of 2013. The total number of PEVs is 15,963 from our simulation, which is close to the actual number from CVRP datasets, 16,103. **b**, Correlation between the simulated PEV and the PEV from CVRP data. **c**,**d**, Probability distributions of commuting distances, *D*, and commuting travel times, *T*, of all vehicle trips and EV trips estimated through income information and trip distances. **e**, Fractions of four types of mobility motif of all commuters and PEV users. 58% of commuters only travel between home and work on weekdays, while the rest 42% have other activities before or after work. Similarly, 66% of commuters using PEVs only travel between home and work, and the rest 34% have other activities before or after work. **f**, Probability distributions of charging energy E_s obtained from charging sessions compared to those of the energy demand estimated by energy consumption model on three charging behaviour scenarios, morning, daily and two-days. **g**, Probability distributions of charging energy E_s and those of the daily energy demand of simulated PEVs for the ZIP codes that have the most charging session records.

therefore, they are limited to accept the recommendations of a time-shift strategy if the recommendation falls before their usual arrival and departure times. Namely, we impose the following restrictions per motif ID. (1) Home-work-home, can change both of the arrival and departure time; (2) home-work-other-home, indicates activities after work, and they can not delay their departure time; (3) home-other-work-home, which indicates activities before work, and they can not change their arrival time; (4) home-other-work-other-home, which indicates the PEV drivers can change neither the arrival nor the departure time.

Figure 5c contrasts the estimates of peak saving with and without the consideration of individual mobility constraints in the optimization strategy, looking at the percentage of peak loads of three schemes with variant *d*. The three schemes are (i) the optimal strategy, where all PEV drivers can follow the time shifts; (ii) the motif blind subtracts to the optimal estimates, all the PEV drivers that will not accept the recommendations due to the individual mobility constraints; (iii) the motif aware is a customized strategy informed by the individual mobility constraints to distribute the time shifts. These three strategies are evaluated under the

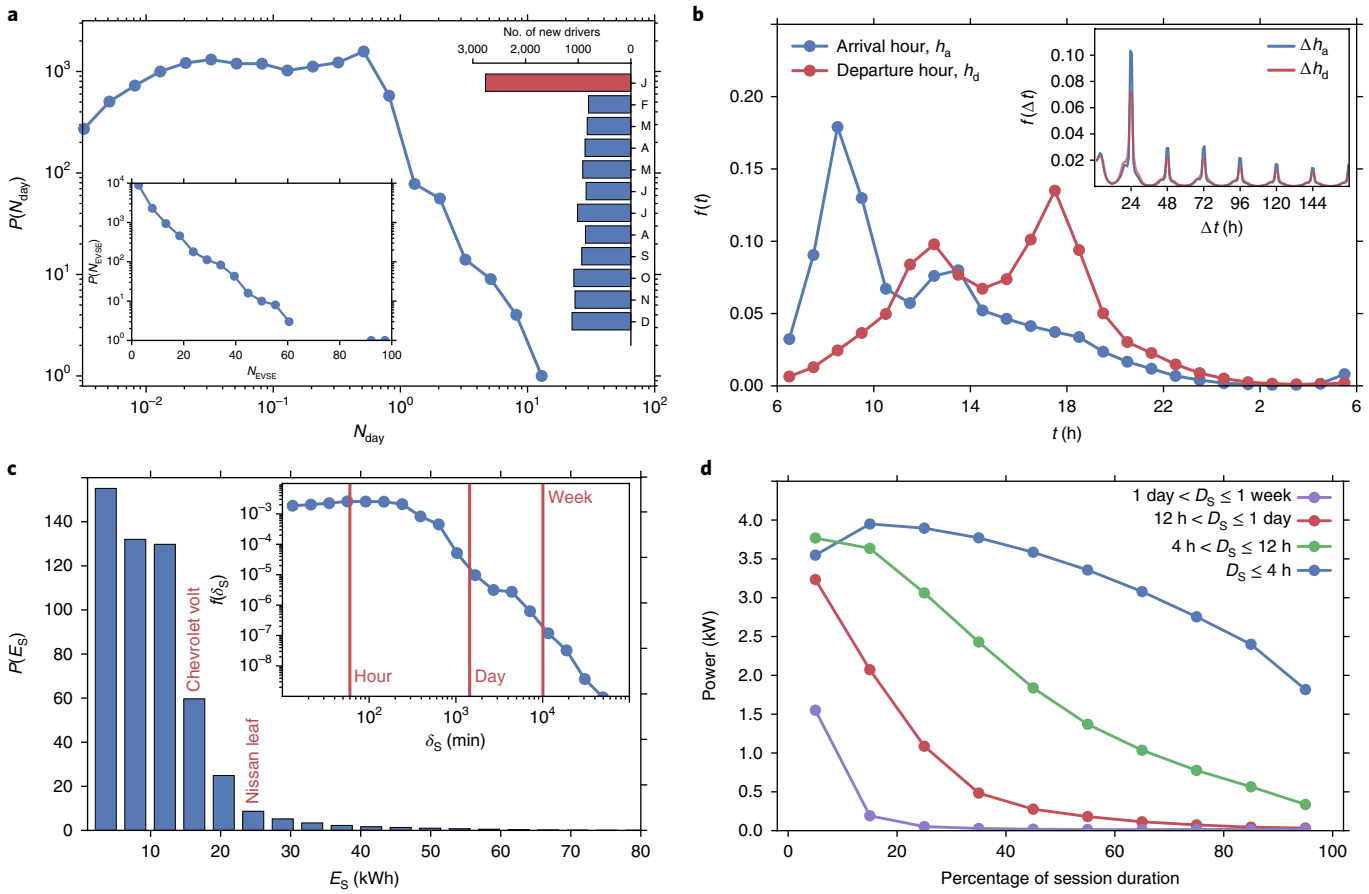

Fig. 4 | PEV charging session profiles. a, Distribution of N_{day}, the number of sessions per day for each driver ID starting from the day of first record (right inset: number of new driver IDs added every month; left inset, distribution of N_{EVSE}, the number of unique EVSEs visited by every driver ID). **b**, Distributions of h_a and h_d, the arrival and departure hours to and from an EVSE. (Inset, the distributions of Δh_a and Δh_d, the inter-arrival and inter-departure times for a driver ID visiting a specific EVSE.) **c**, Distribution of E_S, the total energy withdrawn per session. The battery capacities of the two most commonly used PEVs, Nissan Leaf and Chevrolet Volt, are labelled. (Inset, the distribution of δ_S, session durations. The sessions lasting one hour, one day, and one week are highlighted with red vertical lines.) **d**, Power consumption as a function of the normalized session duration segmented by total duration groups.

end bound and flexible schemes. The comparisons of the power curves of the three schemes and the two strategies are shown in Supplementary Figs. 7 and 8.

The optimal results are the best case scenario because all sessions can be shifted. The motif aware scheme represents the more feasible gains by coupling the charging strategies with the constraints of the drivers. The motif blind scheme is added to show how optimization strategies based on charging data only overestimate the benefits of the savings from 3% to 15%, while this loss can be overcome with the mobility information.

For the motif aware scheme, we examine the peak load saving versus the PEV driver's adoption rate (also known as flexibility) of the time shifts. Figure 5d shows a linear relationship between the acceptance rate and the savings for both of the motif blind and motif aware schemes. With the increase of adoption rate, motif aware contributes more on peak load saving than motif blind. For instance, when 80% of PEV drivers accept the time-shift recommendations, the motif aware scheme reduces the peak load by 424 kW on average, while the motif blind scheme reduces 279 kW on average.

In Fig. 5e, we present the peak load saving of the three flexible schemes versus the number of PEVs travelling to the selected ZIP code. The inset of Fig. 5e shows the estimated peak load without energy demand management. Both the peak load and the three saving powers grow linearly with the numbers of PEVs. The gap between optimal and motif aware is negligible in comparison with optimal versus motif blind.

This framework allows us to evaluate how the time shifts in their departures affect the commuting travel times of the PEV trips into the subject ZIP code. Figure 5f shows that the peak load reductions can be achieved without causing major discomfort to commuters in terms of travel times. The most negatively influenced drivers end up losing a maximum of 20 min in the case of $d=4$ (1 h), and are far less than those who are unaffected by the proposed changes. There is a number of drivers that even achieve travel time savings.

Finally, we examine the monetary outcomes of the proposed strategies, end bound and flexible. We use the max part-peak demand summer rates in the E-19 rate structure for the region to calculate the change in demand charge as a proxy of the cost in terms of dollars[32,52]. When implemented, the possible benefits of the schemes we proposed are displayed in Fig. 5g: monthly potential savings in the demand charge can reach up to US$2,500 for the motif customized and flexible strategy, corresponding to roughly US$5.6 per month per session. Without managing charging, these savings remain unrealized, and are paid by PEV drivers or the companies that subsidize the charging activity. As a sum the savings are substantial, yet for the number of sessions on a typical weekday considered here, the amount saved per individual is relatively small, making the uniform distribution of savings a relatively unexciting reward for cooperation. However, as the

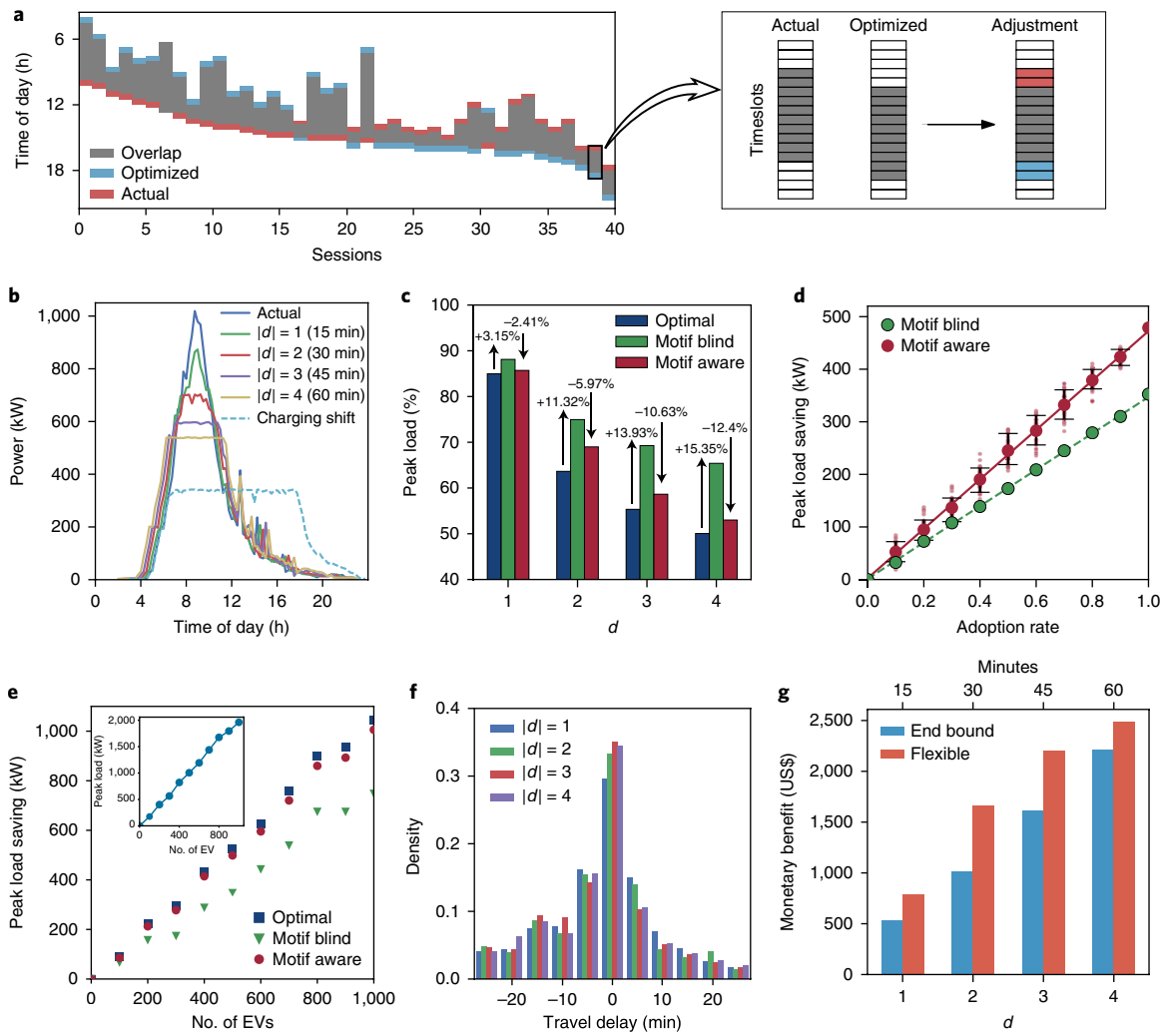

Fig. 5 | Assessing the benefits of minimizing peak power. a, An illustration of 40 sessions during one day in the flexible strategy. The sessions are shifted earlier or later such that the overall peak power is minimized. **b**, Decrease in peak power measurements for the varying d of the flexible and charging-shift strategy. The flexible time shifts are constrained by mobility motifs of PEV users, and the peak shaving of 47% can be achieved. The charging-shift strategy reduces the peak load by 66%. **c**, Percentage peak load of the three schemes 'optimal', 'motif blind' and 'motif aware'. The positive value on the bar implies the gap in the estimates between the optimal versus motif blind, showing the effects of lacking mobility information. The negative value on the bars implies the improvements using motif-aware information versus motif blind, customizing the optimization strategy to the mobility constraints. **d**, Peak-load saving versus PEV driver's adoption rate of the time-shift recommendations, for the motif blind and motif aware schemes when $d=4$. For each adoption rate, we randomly choose PEV drivers who accept the recommendations and average over 50 realizations. The error bar shows the 10th and 90th percentile of the savings of motif aware for the given acceptance rate. The red solid (green dash) line presents the linear fit between the saving of motif aware (blind) and adoption rate. **e**, Projected peak load saving of the flexible strategy when $d=4$ versus the number of PEV users working in the selected ZIP code. The inset shows the projected peak load versus the number of PEV users. **f**, Changes on travel times of morning and evening trips. The majority of the drivers are not influenced, the worst case is a few individuals suffering from additional 20 min delays for $d=4$. **g**, Monthly savings for varying values of d with flexible and end bound strategies.

biggest beneficiary of the PEV traveling management, the power grid operator could pay the PEV drivers to encourage their initiatives on the travel schedule shift. In addition, recent studies have suggested that gamified systems are successful in promoting behaviour that helps achieve social good[53]. More specifically, these systems encourage engagement by building raffles in which each participant has a chance to win a bigger reward with a probability proportional to their cooperation level. This type of mechanism may make incentivization more attractive in the context of PEVs and their electricity demand management.

Moreover, we analyse the potential impact of the PEV travel demand management strategy on the non-EV charging electricity demand in both of the residential regions and commercial buildings. Among the PEV drivers involved in the time-shift strategy, 60% of them are recommended to depart from home earlier and 40% are recommended to depart from home later. Considering most of the household electricity usages have two peaks, morning and evening peak[54], we argue that the time-shift strategy is more likely to relieve the morning peak of electricity usage in the residential area as a part of PEV drivers are leaving home earlier than usual. Similarly, as the PEV drivers arrive home at variant time, the time-shift strategy is also likely to relieve the evening peak load. For the commercial buildings, the power load curve is more stable during the working hours[55]. The change of arrival time to or departure time from the commercial building will have no significant influence on the power load.

Discussion

This work presents an exploratory analysis that couples two unique large datasets on urban mobility and energy consumption of electric vehicles. We address a gap in existing PEV management literature, namely the simplistic modelling of urban mobility, by generating a model of individual mobility informed by large-scale mobile phone data. Moreover, we extend the proposed methodology by demonstrating a charging management scheme and assess its applicability by using the information on individual mobility constraints of the drivers.

We evaluate recommendation schemes of time shifts in the charging sessions constrained by the individual mobility motif of PEV drivers. That is, about 30% of PEV drivers could be limited to change their travel plan due to their schedule in other activities before or after work. Following these, peak power values can be shed by up to 47%. To assess the feasibility of the recommendations, we estimate the possible monetary benefits and the travel time losses resulting from the proposed schemes. The resulting daily savings, while modest at the individual level, are certainly substantial enough to fund game-based prizes that induce cooperation and raise awareness. On the other hand, the travel time losses are almost imperceptible to the majority of the drivers, and a substantial number of drivers, in fact, benefit from the adjustment of their arrival times as it aids them to escape morning traffic.

The presented framework relies on individual location data from mobile phones and a survey of PEV drivers. We designed a Bayesian inference framework to estimate the PEV usage probability of each vehicle driver. The Bayesian inference framework relies on three properties of the PEV users: the distribution of their household income, the distribution of their daily driving distances, and the adoption rate of PEV in the city. While the profiles of PEV adopters may change due to the rebate policy, new battery technique and so on, the surveys can be updated based on sales. Thus, via changing one or more properties, it's easy to estimate the use of PEV in each ZIP code under different scenarios. Associated with the mobility information, the proposed model is adaptable and can be used to evaluate different scenario analysis of future energy demand of PEVs in time and space. In contrast, the prevalent data-driven energy demand methods mainly predict the future demand in a given region with the historical data, which can not estimate long-term consumption under different scenarios[56].

There are various avenues in which this work can be extended. Better understanding of the charging behaviour of PEV drivers and the energy demand in residential regions would complete and enrich our planning estimates. As the PEVs are spreading widely at the moment, a stronger comprehension of the tie among mobility, socioeconomic characteristics of PEV owners and the PEV incentive policies is necessary to accurately grasp the future energy demand as well as the pressure on the power grid. Another interesting avenue is to investigate PEV management when the future energy structure changes, such as the rise of the wind and solar power.

Methods

Datasets. Mobile phone activity data, also known as call detail records (CDRs), have been widely popular in the past decade, especially in the context of mobility modelling[39–41,57–59]. For this work, we make use of the CDRs for the Bay Area including approximately 1.39 million users and more than 200 million calls they made over 6 weeks. Each record contains the anonymized user ID, timestamp, duration and the geographic location of the associated cell tower. The spatial resolution is discretized to the service areas of 892 distinct cell towers. This information is used to build the TimeGeo mobility model for the Bay Area for a typical weekday. More details of the CDRs can be found in ref. [59].

PEV charging profiles provided by ChargePoint (https://www.chargepoint.com), a charging station construction company, contain information on 580,000 PEV charging sessions at commercial PEV supply equipment (EVSE) locations across the Bay Area in 2013. For each charging session, the following information is available: (i) one-time information on the EVSE location type, unique driver ID, total energy transferred and plug-in/plug-out times; and (ii) charging power readings obtained every 15 min. The locations of the charging stations are anonymized to ZIP code level. As a preprocessing step, we filter out those records lasting less than 1 min, not occuring in 2013 or with erroneous power measurements exceeding typical cable capacity and maximum charging rates.

Census and survey information used in this study consists of shapefiles describing census tracts, their population and income information[60]. The survey information is obtained from the California Plug-in Electric Vehicle Driver Survey carried out in 2013[45]. This survey contains information on various sociodemographic characteristics and travel behaviour of PEV drivers in California. We utilize information regarding income and average daily vehicle miles traveled in the estimation of PEV mobility.

Individual mobility model. From the CDRs data, we are able to extract the visited places and time during the period of the dataset for each user. With that information, TimeGeo models and integrates the flexible temporal and spatial mobility choice of the individual. In the model, each day of a week is divided into 144 discrete intervals. For each interval, the individual decides to stay or move, and then where to go if she chooses to move. To represent the movement mechanisms, TimeGeo introduces a time-inhomogeneous Markov chain model with three individual-specific mobility parameters: a weekly home-based tour number (n_w), a dwell rate (β_1) and a burst rate (β_2). $P(t)$ is defined as the global travel circadian rhythm of the population in an average week and it is different for commuters and non-commuters.

For the temporal movement choices, TimeGeo begins with determining if the individual is at home. If true, she will move with probability $n_wP(t)$, which represents her likelihood of making a trip originated from home in a time-interval t of a week. If false, she will move with probability $\beta_1 n_wP(t)$. Then, if she decides to move, she goes to *other* places with probability $\beta_2 n_wP(t)$ and goes back to home with probability $1-\beta_2 n_wP(t)$. The $P(t)$, distribution of n_w, $\beta_1 n_w$ and $\beta_2 n_w$ are illustrated in Supplementary Fig. 3.

For the spatial movement choices, TimeGeo uses a rank-based exploration and preferential return (r-EPR) to determine the next place of the individual. In detail, when the individual chooses to move to another place, she could return to a visited place or explore a new place. The model assumes that the individual explores a new place with probability $P_{new}=\rho S^{-\gamma}$, which captures a decreasing propensity to visit new locations as the number of previously visited locations (S) increases with time. The two parameters, $0<\rho\leq 1$ and $\gamma\geq 0$, are used to control the user's tendency to explore a new location and are calibrated with empirical data. If the individual decides to return, the return location is selected from the visited locations according to her visiting frequency. If she decides to explore a new location, the alternative destinations are selected according to the distance to her origin with probability $P(k)\sim k^{-\alpha}$, where k is the rank of alternative destinations, the one closest to the current location is $k=1$, the second closest $k=2$ and so on, and α is calibrated with the empirical data. More details of the TimeGeo model can be found in ref. [38]. To assess the simulation of individual mobility in Bay Area, we compare the aggregate performance of TimeGeo with NHTS and CHTS and show the results in Fig. 2 and Supplementary Figs. 1 and 2.

Electric vehicle mobility estimation. With the purpose of sampling PEV users from all vehicular drivers in Bay Area, we first extract the vehicular drivers from the entire population with the vehicle usage rate at census tract scale. Then, each vehicular driver is associated with a probability of using PEV, $P(\mathrm{EV}\,|\,I_u, D_u)$ on the basis of the driver's household income I_u and daily driving distance D_u. I_u is the random variable that denotes the income of the trip maker and follows a standard normal distribution centred at the median income of the residential tract. The median income information at tract scale is from census data[60]. $P(I_u)$ is the probability density of the household income of all trip makers in the Bay Area. Similarly, D_u is the random variable that denotes the daily travel distance of the trip maker. The visited locations of the trip maker are obtained from the TimeGeo model and the routing distance is calculated by using a publicly available online API service for routing. $P(D_u)$ is the probability density of the daily travel distance of all travelers in the Bay Area. We assume that for a given trip maker, his or her income I_u and daily travel distance D_u are independent, thereby, $P(I_u, D_u\,|\,\mathrm{EV})=P(I_u\,|\,\mathrm{EV})P(D_u\,|\,\mathrm{EV})$, that is, I_u and D_u are also conditionally independent given a PEV driver.

To estimate the probability of using PEV, $P(\mathrm{EV}\,|\,I_u, D_u)$, we begin by expressing the Bayesian relation:

$$P(\mathrm{EV}|I_u, D_u)=\frac{P(I_u, D_u|\mathrm{EV})P(\mathrm{EV})}{P(I_u, D_u)} \quad (1)$$

By imposing our aforementioned assumptions on equation (1), we have

$$P(\mathrm{EV}|I_u, D_u)=\frac{P(I_u|\mathrm{EV})P(D_u|\mathrm{EV})P(\mathrm{EV})}{P(I_u)P(D_u)} \quad (2)$$

In estimating this value, the share of PEVs within all cars in the Bay Area in 2013 is 0.62% according to the CVRP data[46], that is, $P(\mathrm{EV})=0.62\%$. We make use of the PEV driver survey information regarding income and daily travel distance,

namely $P(I_u|\mathrm{EV})$ and $P(D_u|\mathrm{EV})$, respectively. Once $P(\mathrm{EV}|I_u, D_u)$ is estimated, the probabilities are used to select the PEV drivers from all vehicular drivers. Figure 3c represents the distribution of travel distance in the morning of all vehicular and PEV commuters.

Energy consumption models. We design different energy consumption models for the four popular PEV modes in the Bay Area. In detail, we estimate the power demand of Nissan Leaf with a drivetrain model and the trip information. This drivetrain model builds the relationship between the energy consumption and two aggregate properties of the trip, the average travel speed and the route distance, which we estimate from a publicly available online API service for each PEV trip. That is,

$$E_{\mathrm{trip}}^{\mathrm{Nissan}} = f(V_{\mathrm{trip}})D_{\mathrm{trip}} \tag{3}$$

where V_{trip} and D_{trip} are the average speed and route distance of the trip respectively. $f(V_{\mathrm{trip}})$ implies the consumed power per mile (kWh mile^{-1}) when the PEV is traveling at speed V_{trip} (mile h^{-1}). However, $f(V_{\mathrm{trip}})$ depends on the battery used by the PEV model, meaning that different PEV models show different shapes of $f(V_{\mathrm{trip}})$. In this work, we fit $f(V_{\mathrm{trip}})$ with a piecewise linear function using the data observed from Nissan Leaf[5]. The curve of $f(V_{\mathrm{trip}})$ is given in Supplementary Fig. 6b and the formulation is given as follows:

$$f(V_{\mathrm{trip}}) = \begin{cases} -23.12\times10^{-3}\times V_{\mathrm{trip}} + 0.439 & V_{\mathrm{trip}} \le 6.70 \\ -8.14\times10^{-3}\times V_{\mathrm{trip}} + 0.338 & 6.70 \le V_{\mathrm{trip}} \le 12.71 \\ -0.38\times10^{-3}\times V_{\mathrm{trip}} + 0.240 & 12.71 \le V_{\mathrm{trip}} \le 21.75 \\ 2.11\times10^{-3}\times V_{\mathrm{trip}} + 0.185 & 21.75 \le V_{\mathrm{trip}} \le 60.00 \end{cases} \tag{4}$$

The consumption of Tesla Model S is the estimated by scaling the consumption of Nissan Leaf in the same trip by 1.229, as the Tesla model S consumes 22.9% more energy on average than the Nissan Leaf[51]. That is, $E_{\mathrm{trip}}^{\mathrm{Tesla}} = 1.229 f(V_{\mathrm{trip}})D_{\mathrm{trip}}$.

For the PHEVs, we introduce the charge-depleting models to estimate their energy consumptions,

$$E_{\mathrm{trip}}^{\mathrm{PHEV}} = \min\{D_{\mathrm{trip}}\times r, C_{\mathrm{PHEV}}\} \tag{5}$$

where r and C_{PHEV} are the electricity consumption rate and the battery capacity of the PHEV, respectively. It has been previously calibrated that $r = 0.288$ kWh mile^{-1} for PHEVs with 10 mi electric range; $r = 0.337$ kWh mile^{-1} for PHEVs with 20 mile electric range; and $r = 0.342$ kWh mile^{-1} for PHEVs with 40 mile electric range[49]. In the Bay Area, the two most popular modes of PHEVs are Chevrolet Volt and Toyota Prius, and their electric ranges are 40 and 10 mile, respectively. The energy consumption models used here also match with the EV efficiency ratings released by the US Department of Energy (see Supplementary Table 1).

Optimization model. We begin by discretizing a day into 15-min intervals such that each day starts at $t = 0$ and ends at $t = 95$ (ref. [32]). For each charging session i among N in a day happen in a selected ZIP code, we define t_a^i as the arrival time index, t_c^i as the time index where charging is complete, and t_d^i as the departure time index. We represent the time indices by the vector $\boldsymbol{\tau}^i$, and the power consumption by vectors $\mathbf{P}^i$ and $\mathbf{Q}^i$, all defined as follows:

$$\begin{aligned} \boldsymbol{\tau}^i &= [t_a^i, \ldots, t_c^i]^\top \\ \mathbf{P}^i &= [P_0^i, \ldots, P_{95}^i]^\top \\ \mathbf{Q}^i &= [P_{t_a^i}^i, \ldots, P_{t_c^i}^i]^\top \end{aligned} \tag{6}$$

By shifting $\mathbf{Q}^i$ within $\mathbf{P}^i$ by an amount d^i for all sessions, we can modify the overall power demand curve. We define $M^i = (t_c^i - t_a^i) + 1$ as the total number of non-zero power measurements in this charging session (that is, total number of elements in $\mathbf{Q}^i$), given that charging sessions start immediately on arrival. We enforce continuity of the charging process, the non-violation of departure times and amounts of session energy.

To capture the constraints proposed above, we introduce the following formal constraints:

$$\left.\begin{aligned} &\tau_j^i \ge 0 \\ &\tau_j^i \le 95 \\ &\tau_j^i \ge t_a^i + d^i \\ &\tau_j^i \le t_c^i + d^i \\ &t_d^i \ge t_c^i + d^i \\ &\tau_j^i < \tau_{j+1}^i \end{aligned}\right| \begin{aligned} &\forall i \in [1, N] \\ &\forall j \in [1, M^i] \end{aligned} \tag{7}$$

where d^i is the delay of the charging session of the ith PEV driver. As the mobility motif of the PEV driver limits the acceptability of the recommendations, we customize d^i for the PEV drivers with different mobility motifs as shown in Fig. 3e. Assuming that the delay of strategy is d, we introduce the following constraints:

$$d^i = \begin{cases} d & \mathrm{H-W-H} \\ \min\{0, d\} & \mathrm{H-W-O-H} \\ 0 & \mathrm{H-O-W-H\ \&\ H-O-W-O-H} \end{cases} \tag{8}$$

In this customization of delay, the drivers with mobility motif 'home-work-home' (H-W-H) could accept any change of arrival and departure time; the drivers with mobility motif 'home-work-other-home' (H-W-O-H) can not delay their departure time, that is, the delay d must be non-positive; the drivers with mobility motif 'home-other-work-home' (H-O-W-H) can not change their arrival time; the drivers with mobility motif 'home-other-work-other-home' (H-O-W-O-H) can change neither their arrival time nor departure time.

We construct the proposed constraints using a binary decision matrix to represent charging or non-charging time slots within the optimization duration. To represent the candidate time slot at which Q_j^i can be positioned, we create binary row vectors $\boldsymbol{x}_j^i$ each consisting of 95 binary decision variables: $x_{j,k}^i \in \{0,1\}$, $\forall j \in [1, M^i]$, $\forall i \in [1, N]$, $\forall k \in [0, 95]$.

$$\mathbf{X}^i = \begin{bmatrix} \mathbf{x}_1^i \\ \vdots \\ \mathbf{x}_{\mathbf{M}^i}^i \end{bmatrix} = \begin{bmatrix} x_{1,0}^i & & x_{1,95}^i \\ \vdots & \ddots & \vdots \\ x_{M^i,0}^i & & x_{M^i,95}^i \end{bmatrix} \tag{9}$$

Finally, we write the variables in the constraints given in equation (7) using the binary decision variable as follows:

$$\boldsymbol{\tau}^i = \mathbf{X}^i \begin{bmatrix} 0 \\ \vdots \\ 95 \end{bmatrix} \tag{10}$$

The aggregate power vector $\mathbf{AP}$ is given as follows:

$$\mathbf{AP} = \sum_{i=0}^{N} \mathbf{P}^i = \begin{bmatrix} \mathbf{Q}^1 \\ \vdots \\ \mathbf{Q}^N \end{bmatrix}^\top \begin{bmatrix} \mathbf{X}^1 \\ \vdots \\ \mathbf{X}^N \end{bmatrix} \tag{11}$$

The resulting formulation is a mixed-integer linear program, with decision variables $\boldsymbol{X}^i$, P_{peak} and d^i of which the latter two are integers. The problem can be proposed to minimize the daily peak load P_{peak} for a group of PEVs arriving to the same ZIP code location, subject to equation (7) and the following additional constraints:

$$\mathrm{AP}_t^i \le P_{\mathrm{peak}}, \forall i \in [1, N], \forall t \in [0, 95] \tag{12}$$

Data availability. All data needed to evaluate the conclusions in the paper are present in the paper. Additional data related to this paper may be requested from the authors.

Received: 24 May 2016; Accepted: 19 March 2018;
Published online: 30 April 2018

References

1. Michalek, J. J. et al. Valuation of plug-in vehicle life-cycle air emissions and oil displacement benefits. *Proc. Natl Acad. Sci. USA* **108**, 16554–16558 (2011).
2. Atia, R. & Yamada, N. More accurate sizing of renewable energy sources under high levels of electric vehicle integration. *Renew. Energy* **81**, 918–925 (2015).
3. Needell, Z. A., McNerney, J., Chang, M. T. & Trancik, J. E. Potential for widespread electrification of personal vehicle travel in the united states. *Nat. Energy* **1**, 16112 (2016).
4. Nykvist, B. & Nilsson, M. Rapidly falling costs of battery packs for electric vehicles. *Nat. Clim. Change* **5**, 329–332 (2015).
5. Melton, N., Axsen, J. & Sperling, D. Moving beyond alternative fuel hype to decarbonize transportation. *Nat. Energy* **1**, 16013 (2016).
6. Hu, X., Moura, S. J., Murgovski, N., Egardt, B. & Cao, D. Integrated optimization of battery sizing, charging, and power management in plug-in hybrid electric vehicles. *IEEE Trans. Control Syst. Technol.* **24**, 1036–1043 (2016).
7. DeShazo, J. Improving incentives for clean vehicle purchases in the united states: challenges and opportunities. *Rev. Environ. Econ. Policy* **10**, 149–165 (2016).
8. *Global EV Outlook: Understanding the Electric Vehicle Landscape to 2020* (International Energy Agency, 2013).
9. Hines, P., Apt, J. & Talukdar, S. Large blackouts in North America: historical trends and policy implications. *Energy Policy* **37**, 5249–5259 (2009).

10. Brummitt, C. D., Hines, P. D., Dobson, I., Moore, C. & D'Souza, R. M. Transdisciplinary electric power grid science. *Proc. Natl Acad. Sci. USA* **110**, 12159–12159 (2013).
11. Buldyrev, S. V., Parshani, R., Paul, G., Stanley, H. E. & Havlin, S. Catastrophic cascade of failures in interdependent networks. *Nature* **464**, 1025–1028 (2010).
12. Brummitt, C. D., D'Souza, R. M. & Leicht, E. Suppressing cascades of load in interdependent networks. *Proc. Natl Acad. Sci. USA* **109**, E680–E689 (2012).
13. Pahwa, S., Scoglio, C. & Scala, A. Abruptness of cascade failures in power grids. *Sci. Rep.* **4**, 3694 (2014).
14. McAndrew, T. C., Danforth, C. M. & Bagrow, J. P. Robustness of spatial micronetworks. *Phys. Rev. E* **91**, 042813 (2015).
15. Mwasilu, F., Justo, J. J., Kim, E.-K., Do, T. D. & Jung, J.-W. Electric vehicles and smart grid interaction: A review on vehicle to grid and renewable energy sources integration. *Renew. Sustain. Energy Rev.* **34**, 501–516 (2014).
16. Halu, A., Scala, A., Khiyami, A. & González, M. C. Data-driven modeling of solar-powered urban microgrids. *Sci. Adv.* **2**, e1500700 (2016).
17. Mureddu, M., Caldarelli, G., Chessa, A., Scala, A. & Damiano, A. Green power grids: how energy from renewable sources affects networks and markets. *PLoS ONE* **10**, e0135312 (2015).
18. Bayram, I. S., Michailidis, G., Devetsikiotis, M., Granelli, F. & Bhattacharya, S. *Control and Optimization Methods for Electric Smart Grids* 133–145 (Springer, New York, 2012).
19. Callaway, D. S. & Hiskens, I. A. Achieving controllability of electric loads. *Proc. IEEE* **99**, 184–199 (2011).
20. Moura, S. J., Fathy, H. K., Callaway, D. S. & Stein, J. L. A stochastic optimal control approach for power management in plug-in hybrid electric vehicles. *IEEE Trans. Control Syst. Technol.* **19**, 545–555 (2011).
21. Clement-Nyns, K., Haesen, E. & Driesen, J. The impact of charging plug-in hybrid electric vehicles on a residential distribution grid. *IEEE Trans. Power Syst.* **25**, 371–380 (2010).
22. Tal, G., Nicholas, M., Davies, J. & Woodjack, J. Charging behavior impacts on electric vehicle miles traveled: who is not plugging in? *Transp. Res. Rec.* **2454**, 53–60 (2014).
23. Harris, C. B. & Webber, M. E. An empirically-validated methodology to simulate electricity demand for electric vehicle charging. *Appl. Energy* **126**, 172–181 (2014).
24. Lin, Z. Optimizing and diversifying electric vehicle driving range for US drivers. *Transp. Sci.* **48**, 635–650 (2014).
25. Rajakaruna, S., Shahnia, F. & Ghosh, A. *Plug In Electric Vehicles in Smart Grids* (Springer, Singapore, 2015).
26. Tamor, M. A., Moraal, P. E., Reprogle, B. & Milačić, M. Rapid estimation of electric vehicle acceptance using a general description of driving patterns. *Transp. Res. C* **51**, 136–148 (2015).
27. Hines, P. et al. *Understanding and Managing the Impacts of Electric Vehicles on Electric Power Distribution Systems* (Univ. Vermont, 2014).
28. Yuksel, T. & Michalek, J. J. Effects of regional temperature on electric vehicle efficiency, range, and emissions in the united states. *Environ. Sci. Technol.* **49**, 3974–3980 (2015).
29. Rezaei, P., Frolik, J. & Hines, P. D. Packetized plug-in electric vehicle charge management. *IEEE Trans. Smart Grid* **5**, 642–650 (2014).
30. Valogianni, K., Ketter, W., Collins, J. & Zhdanov, D. Effective management of electric vehicle storage using smart charging in *Proc. 28th AAAI Conf. Artif. Intel.* 472–478 (2014).
31. Ma, Z., Callaway, D. S. & Hiskens, I. A. Decentralized charging control of large populations of plug-in electric vehicles. *IEEE Trans. Control Syst. Technol.* **21**, 67–78 (2013).
32. Kara, E. C. et al. Estimating the benefits of electric vehicle smart charging at non-residential locations: a data-driven approach. *Appl. Energy* **155**, 515–525 (2015).
33. Subramanian, A., Garcia, M. J., Callaway, D. S., Poolla, K. & Varaiya, P. Real-time scheduling of distributed resources. *IEEE Trans. Smart Grid* **4**, 2122–2130 (2013).
34. Yang, L., Zhang, J. & Poor, H. V. Risk-aware day-ahead scheduling and real-time dispatch for electric vehicle charging. *IEEE Trans. Smart Grid* **5**, 693–702 (2014).
35. Zakariazadeh, A., Jadid, S. & Siano, P. Multi-objective scheduling of electric vehicles in smart distribution system. *Energy Convers. Manag.* **79**, 43–53 (2014).
36. Garca-Villalobos, J., Zamora, I., San Martn, J., Asensio, F. & Aperribay, V. Plug-in electric vehicles in electric distribution networks: A review of smart charging approaches. *Renew. Sustain. Energy Rev.* **38**, 717–731 (2014).
37. Alizadeh, M. et al. Optimal pricing to manage electric vehicles in coupled power and transportation networks. *IEEE Trans. Control Netw. Syst.* **4**, 863–875 (2016).
38. Jiang, S. et al. The TimeGeo modeling framework for urban mobility without travel surveys. *Proc. Natl Acad. Sci. USA* **113**, E5370–E5378 (2016).
39. Jiang, S. et al. A review of urban computing for mobile phone traces: current methods, challenges and opportunities. In *Proc. 2nd ACM SIGKDD Int. Worksh. Urban Computing* 2 (ACM, 2013).
40. Çolak, S., Alexander, L. P., Alvim, B. G., Mehndiratta, S. R. & González, M. C. Analyzing cell phone location data for urban travel: current methods, limitations, and opportunities. *Transp. Res. Rec.* **2526**, 126–135 (2015).
41. Toole, J. L. et al. The path most traveled: travel demand estimation using big data resources. *Transp. Res. Part C* **58**, 162–177 (2015).
42. *Transportation Secure Data Center* (National Renewable Energy Laboratory, accessed 15 January 2015); http://www.nrel.gov/tsdc
43. *National Household Travel Survey* (US Department of Transportation, Federal Highway Administration, accessed 1 October 2016); http://nhts.ornl.gov
44. Schneider, C. M., Belik, V., Couronné, T., Smoreda, Z. & González, M. C. Unravelling daily human mobility motifs. *J. R. Soc. Interface* **10**, 20130246 (2013).
45. *California Plug-in Electric Vehicle Driver Survey Results: May 2013* (California Center for Sustainable Energy, 2013).
46. *California Air Resources Board Clean Vehicle Rebate Project, Rebate Statistics* (Center for Sustainable Energy, accessed 5 April 2017); https://cleanvehiclerebate.org/rebate-statistics
47. *Commute Time* (Vital Signs, accessed 16 May 2017); http://www.vitalsigns.mtc.ca.gov/commute-time
48. Saxena, S., Floch, C. L., MacDonald, J. & Moura, S. Quantifying EV battery end-of-life through analysis of travel needs with vehicle powertrain models. *J. Power Sources* **282**, 265–276 (2015).
49. Wu, X., Dong, J. & Lin, Z. Cost analysis of plug-in hybrid electric vehicles using GPS-based longitudinal travel data. *Energy Policy* **68**, 206–217 (2014).
50. Yilmaz, M. & Krein, P. T. Review of battery charger topologies, charging power levels, and infrastructure for plug-in electric and hybrid vehicles. *IEEE Trans. Power Electron.* **28**, 2151–2169 (2013).
51. *Workplace Charging Challenge, Mid-program Review: Employees Plug in* (US Department of Energy, 2015).
52. *Electric Schedule e-19: Medium General Demand-metered TOU Service* (Pacific Gas and Electric Company, 2010).
53. Merugu, D., Prabhakar, B. S. & Rama, N. An incentive mechanism for decongesting the roads: A pilot program in bangalore. *Proc. ACM NetEcon Worksh.* (ACM, 2009).
54. Xu, S., Barbour, E. & González, M. C. Household segmentation by load shape and daily consumption. *Proc. 6th ACM SIGKDD Int. Worksh. Urban Computing,* 2 (ACM, 2017).
55. Luo, X., Hong, T., Chen, Y. & Piette, M. A. Electric load shape benchmarking for small-and medium-sized commercial buildings. *Appl. Energy* **204**, 715–725 (2017).
56. Xydas, E. et al. A data-driven approach for characterising the charging demand of electric vehicles: a UK case study. *Appl. Energy* **162**, 763–771 (2016).
57. Blondel, V. D., Decuyper, A. & Krings, G. A survey of results on mobile phone datasets analysis. *EPJ Data Sci.* **4**, 10 (2015).
58. Alexander, L., Jiang, S., Murga, M. & González, M. C. Origin-destination trips by purpose and time of day inferred from mobile phone data. *Transp. Res. Part C* **58**, 240–250 (2015).
59. Çolak, S., Lima, A. & González, M. C. Understanding congested travel in urban areas. *Nat. Commun.* **7**, 10793 (2016).
60. *Census Data* (United States Census Bureau, accessed 15 October 2016); https://www.census.gov/data.html
61. Fiori, C., Ahn, K. & Rakha, H. A. Power-based electric vehicle energy consumption model: Model development and validation. *Appl. Energy* **168**, 257–268 (2016).

Acknowledgements

We would like to thank ChargePoint for providing the electric vehicle charging data and Airsage for providing the call detail records used in this study. We also would like to thank S. Kiliccote and M. Tabone for their valuable feedback. This work was supported by the Siebel Energy Institute and MIT Energy Initiative.

Author contributions

Y.X., S.C. and E.C.K. conceived the research and designed the analyses. Y.X., S.C. and M.C.G. performed the analyses and wrote the paper. S.J.M. and M.C.G. provided general advice and supervised the research.

Competing interests

The authors declare no competing interests.

Additional information

Supplementary information is available for this paper at https://doi.org/10.1038/s41560-018-0136-x.

Reprints and permissions information is available at www.nature.com/reprints.

Correspondence and requests for materials should be addressed to M.C.G.

Publisher's note: Springer Nature remains neutral with regard to jurisdictional claims in published maps and institutional affiliations.